Agricultural Water Management 256 (2021) 107068

Contents lists available at ScienceDirect

Agricultural Water Management

journal homepage: www.elsevier.com/locate/agwat

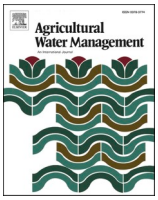

Forecasting of applied irrigation depths at farm level for energy tariff periods using Coactive neuro-genetic fuzzy system

R. González Perea *, E. Camacho Poyato, J.A. Rodríguez Díaz

Department of Agronomy (Unit of Excellence María de Maeztu), University of Córdoba, Campus Rabanales, Edif. da Vinci, 14071 Córdoba, Spain

ARTICLE INFO

Handling Editor: J.E. Fernández

Keywords:
Irrigation scheduling
Artificial intelligence
CANFIS
Genetic algorithm
Farmer's behaviour modelling

ABSTRACT

Nowadays, water scarcity and the increase in energy demand and their associated costs in pressurized irrigation systems are causing serious challenges. In addition, most of these pressurized irrigation systems has been designed to be operated on-demand where irrigation water is continuously available to farmers complexing the daily decision-making process of the water user association' managers. Know in advance how much water will be applied by each farmer and its distribution during the day would facilitate the management of the system and would help to optimize the water use and energy costs. In this work, a new hybrid methodology (CANGENFIS) combining Multiple input -Multiple output, fuzzy logic, artificial neural networks and multiobjective genetic algorithms was developed to model farmer behaviour and short-term forecasting the distribution by tariff period of the irrigation depth applied at farm level. CANGENFIS which was developed in Matlab was applied to a real water user association located in Southwest Spain. Three optimal models for the main crops in the water user association were obtained. The average for all tariff periods of the representability (R^2) and accuracy of the forecasts (standard error prediction, SEP) were 0.70, 0.76% and 0.85% and 19.9%, 22.9% and 19.5%, for rice, maize and tomato crops models, respectively.

1. Introduction

Irrigated agriculture uses nearly 70% of the total water consumption in the world (Conforti, 2011). This value accounts for up to 90% of the total water resources in arid developing countries (Bazilian et al., 2011). In Europe, irrigated agriculture uses around 33% of total water used although this figure may reach over 80% in Southern Europe countries (EEA, 2012) and in the whole Mediterranean region. Thus, efficient water use is essential in a sustainable agricultural system because of reduced water availability (Hunt, 2004) mainly in arid and semi-arid regions like Spain.

In Spain, after a National Modernization Plan of Irrigation (MARM, 2010) water use efficiency was improved replacing the obsolete open-channel distribution systems by pressurize networks (Plusquellec, 2009). However, despite of the upgrading of these water distribution systems allowed to reduce the water used by 21%, the energy consumption per unit area was risen by 657% (Corominas, 2010) which may lead to additional costs for farmers that may be unable to afford such expense if their production is devoted to low-value crops. On the other hand, because of this modernization processes, most of the new irrigation systems were designed to be operated on-demand where water is continuously available to farmers who are free to decide how and when irrigate. Although the increased operation flexibility is a positive aspect for farmers, the management of the whole water distribution system is a more complex task because the hydraulic systems must work under a wide range of operating conditions, in terms of flow and pressure. In addition, since the liberalization of the Spanish Electricity Market, on 1st January 2008, the special tariffs for irrigation disappeared and now, Water Users Associations (WUA) are subject to the general industrial tariffs whose prices vary along the day and the irrigation season.

Under this scenario of water scarcity, the increase in energy demand of the new pressurized irrigation systems, the uncertainty associated with irrigation water demand and the liberalization of the electricity market are causing serious challenges in the daily management of the WUAs. Related to this, water demand forecasting could be one of the main tools to improve the management of the WUAs and help managers in the daily decision-making processes.

The recent revolution of the Information and Communication Technologies (ICTs), as well as the development of new low-cost sensors

* Corresponding author.
E-mail addresses: g72goper@uco.es (R. González Perea), ag1capoe@uco.es (E. Camacho Poyato), jarodriguez@uco.es (J.A. Rodríguez Díaz).

https://doi.org/10.1016/j.agwat.2021.107068
Received 5 May 2021; Received in revised form 28 June 2021; Accepted 7 July 2021
Available online 15 July 2021

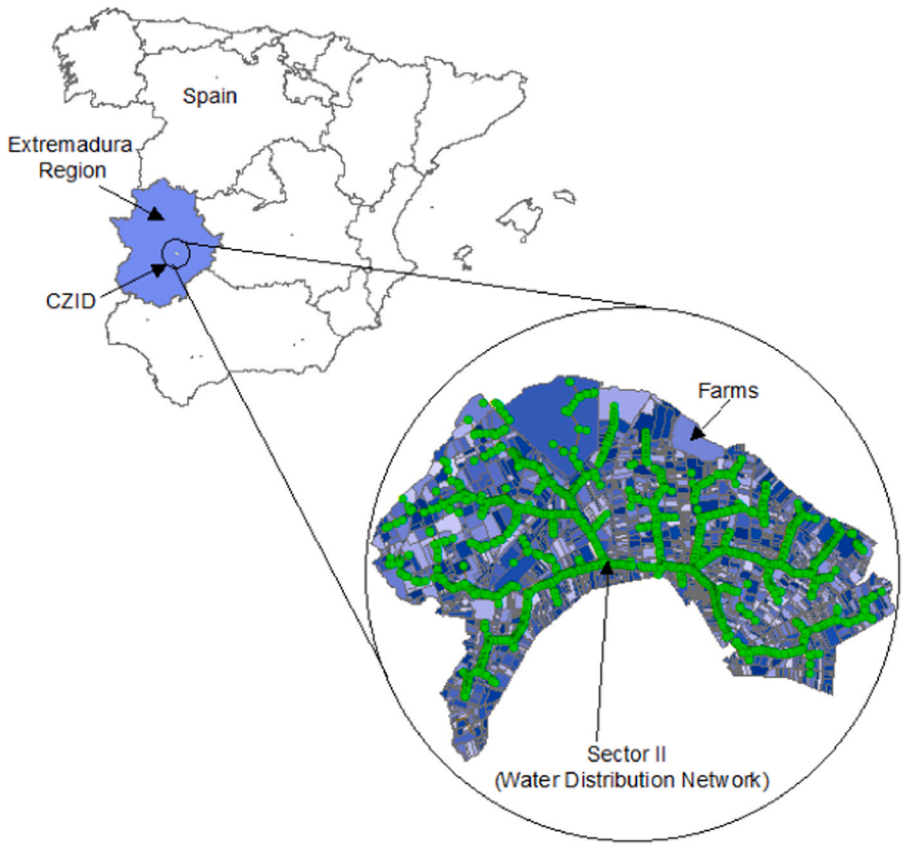

Fig. 1. Location of Sector II of the Canal del Zújar Irrigation District (CZID).

capable to automatically collect thousands of robust data of the whole water-soil-plant-atmosphere system, has modified the technological environment of the current agriculture. The available technology offers new possibilities for the water demand forecasting that may lead to better water and energy use efficiencies, making the WUAs more sustainable, in environmental, social and economic aspects. In addition, the Cloud computing development and virtual storage has reduced the storage cost of Big Data (Bin and Xin, 2013). Thus, the synergism of techniques of Artificial Intelligence (AI) such as Artificial Neural Networks (ANNs), Fuzzy Logic (FL) and Genetic Algorithms (GAs) allow soft computing to incorporate human knowledge effectively, deal with imprecisions and uncertainty, and design adaptation strategies for improve the WUA management.

AI techniques have been applied to solve different problems of water resources management and planning such as: modelling monthly, daily and hourly rainfall-runoff process (Agarwal et al., 2006; Anctil and Rat, 2005), real-time river level and lake stage forecasting (Ondimu and Murase, 2007) or the optimization of the multi-crop pattern plan using Fuzzy Logic and Genetic Algorithms (Rezaei et al., 2017). Previous research also works focused on the prediction of water demand at irrigation district level, using neuro-genetic algorithms (González Perea et al., 2015; Pulido-Calvo and Gutiérrez-Estrada, 2009). However, forecasting water demand at individual farmer level is an extremely complex task. Forecasting of the farmer's behavior was addressed by González Perea (2017) and González Perea et al. (2018). Two models were developed to predict the occurrence of the irrigation events (González Perea, 2017) and the daily applied irrigation depth (González Perea et al., 2018), respectively. However, an optimal daily decision making in WUAs requires not only the knowledge of the of irrigation events occurrence and the applied irrigation depths but their hourly distribution. Since electricity tariffs are organized in hourly periods, the knowledge of the hourly distribution of water consumption would be useful for the optimal contracting of these tariffs.

In this work, a hybrid model combining Multiple-input Multiple output (MIMO) of an Adaptive Neuro Fuzzy Inference System (ANFIS) known as Co-active Neuro-Fuzzy Inference System (CANFIS) has been developed to forecast one-day ahead the distribution in energy tariff periods of the irrigation depths applied at farm level. CANFIS has been optimized by the multiobjective GA NSGA-II (Deb et al., 2002). The model which was developed in Matlab™ and integrated as toolbox was validated and tested in a real WUA.

2. Study area and data source

Canal del Zújar Irrigation District (CZID) (Fig. 1) was selected as real WUA to validate and test the forecast model developed in this study. The model was trained and tested with data from the 2015, 2016, 2017 and 2018 irrigation seasons. This WUA, located in Southwest Spain (Extremadura region), is made up of 10 independent hydraulic sectors covering a total area of 21141 ha. The closest weather station is "Don Benito-EFA" (UTM coordinates (x, y, zone): 252468, 431917, 30). The average temperature in the area ranges from 7.1 °C in January to 25 °C in July, and the average maximum temperature ranges from 13.2 °C to 35.1 °C. The average relative humidity ranged from 30.06% to 99.8%, with a mean value of 66.17% and a standard deviation of 17.30%. The average annual rainfall is 390 mm, with an average daily value of 1.03 mm but with maximum daily values that reach 20 mm The average wind speed ranged from 0.25 m s^{-1} to 7.43 m s^{-1} for the studied seasons. The maximum evapotranspiration occurs in July, with a daily average value of 7.03 mm and peak values around 9 mm. The average annual evapotranspiration is 1296 mm.

Sector II was selected for this work because of the high amount of available data. This sector covers an irrigated area of 2691 ha and is composed of 191 hydrants with a nominal pressure at each hydrant of

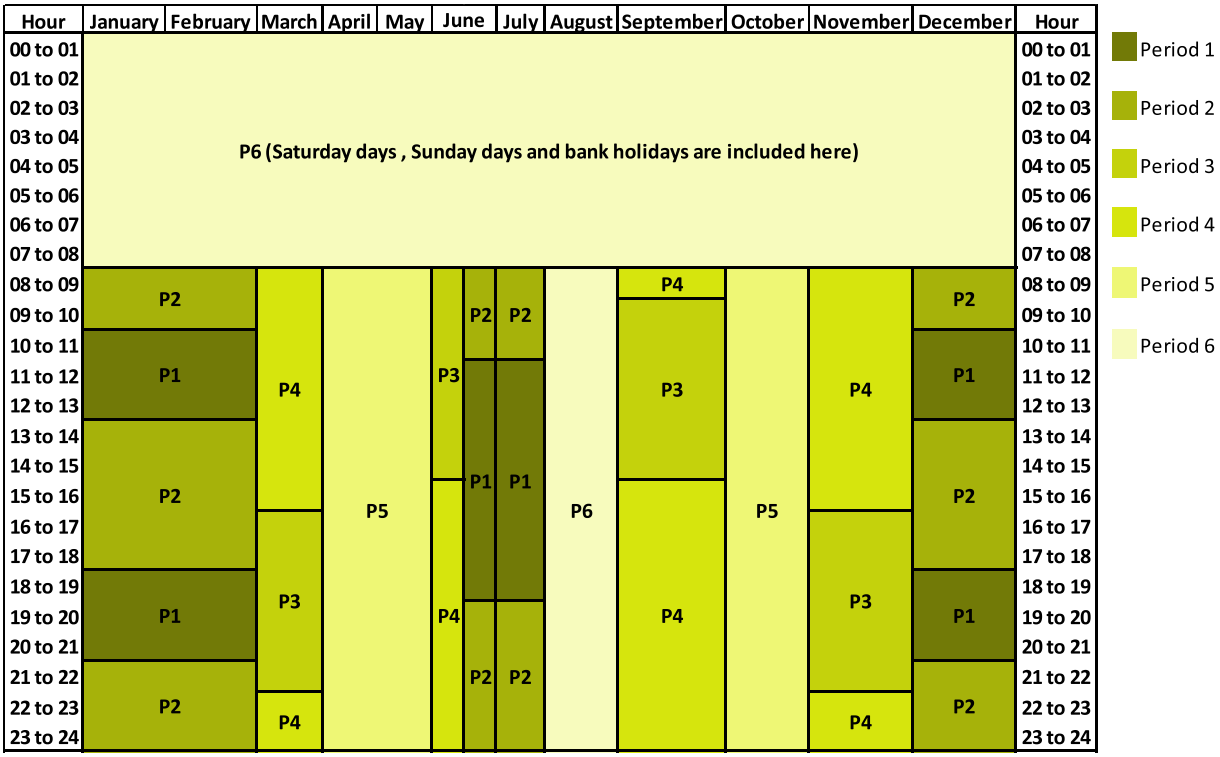

Fig. 2. Temporal distribution of the electrical tariff according to its price in CZID.

25 m. The main crops are tomato, maize and rice (90% of the total irrigated area). The number of samples (water depth records) of each crop was 54,475, 18,568 and 4451, for tomato, maize and rice, respectively. Drip irrigation is used for tomato and maize, while rice is flood irrigated. The typical annual irrigation needs for these crops of this WUA are 6110 m3 ha^{-1}, 5950 m^3 ha^{-1} and 11,103 m^3 ha^{-1}, respectively. The average and standard deviation of the area of the farms are 1.15 ha and 2.08 ha, respectively. However, the largest farm covers an area of 26 ha. Sector II of the CZID has a remote telemetry system which records every hour the volume of water applied in each hydrant. In addition, for each hydrant information about supplied farm and crops are also recorded. The electrical tariff in this WUA is organized in six periods, being period 1 (P1) the most expensive period and period 6 (P6) the cheapest one. Fig. 2 shows the temporal distribution of each period along the irrigation season.

3. Methodology

3.1. Model inputs identification

A previous step to generate the hybrid model is needed to reduce the dimension of the input space and identify the significant inputs from the full set of possible inputs. There are many techniques to achieve this inputs space reduction. Principal components analysis or partial least square cardinal components are two of these techniques widely used. However, when the significant input variables resulting from these techniques are used in nonlinear models, very poor results are usually got (Lin et al., 1996). Therefore, an adaptation of the methodology developed by Lin et al. (1996) has been used in this work to identify the significant inputs. Lin et al. (1996) determined automatically the most significant inputs for a single output variable using fuzzy curves and fuzzy surfaces. Because of the MIMO (Multiple input -Multiple output) nature of the hybrid model developed in this work, an extension N dimensional of the fuzzy curves and fuzzy surfaces have been developed. Thus, the fuzzy curves have been extended to a beam of N-fuzzy and fuzzy surfaces have been transformed to N-dimensional fuzzy curves. The number of output variables of the predictive model defined the N-dimensionality of the fuzzy curves and surfaces.

For a potential input variable *iv*, PI_{iv}, fuzzy curve beams, $c_{iv,ov}$,are created (Eq. (1)). Each curve determined the relationship between *iv* and the output variable *ov* of the forecasting model (DWA_{ov}, daily amount of water applied by each farmer in the energy tariff period *ov*).

$$c_{iv,ov}(PI_{iv}) = \frac{\sum_{k=1}^{M_{ov}} DWA_{k:ov} \bullet \mu_{iv,k:ov}(PI_{iv})}{\sum_{k=1}^{M_{ov}} \mu_{iv,k:ov}(PI_{iv})} \quad ,for\ ov = 1,\ldots,N_{ov} \tag{1}$$

where $\mu_{iv,\,k:ov}$ is the fuzzy membership function of point *k* in the space *iv*-DWA_{ov} which relates the potential input variable *iv* and the daily amount of water applied by each farmer in the energy tariff period *ov* and it is defined by Eq. (2); M_{ov} is the total number of points in the space PI_{iv}-DWA_{ov}; $DWA_{k:ov}$ is the daily amount of water applied by each farmer in point *k* of the space PI_{iv}- DWA_{ov} and N_{ov} is the total number of output variables of the forecast model.

$$\mu_{iv,k:ov}(PI_{iv}) = \exp\left(-\left(\frac{PI_{iv,k:ov} - PI_{iv}}{b}\right)^2\right), \quad for\ ov = 1,\ldots,N_{ov} \tag{2}$$

where $PI_{iv,k:ov}$ is the value of PI_{iv} at point *k* in the space PI_{iv}-DWA_{ov} and *b* takes a value close to two (Lin et al., 1996).

Hereafter, the mean square error values, *MSE*, of each $c_{iv,ov}$ curve are computed and sorted in ascending order according to Eq. (3). If there is a fully random relationship between the input variable *iv* and the DWA_{ov}, the fuzzy curves is flat and the $MSEc_{iv,ov}$ is large. Otherwise, $MSEc_{iv,ov}$ takes small values when the relationship in the space PI_{iv}-DWA_{ov} is more significant.

$$\mathrm{MSE}_{c_{iv,ov}} = \frac{1}{M_{ov}} \sum_{k=1}^{M_{ov}} \left(c_{iv,k:ov}(PI_{iv}) - DWA_{k:ov}\right)^2 \quad ,for\ ov = 1,\ldots,N_{ov} \tag{3}$$

According to Lin et al. (1996), a fuzzy surface is a space with a two-dimensional fuzzy curve. In this work, a fuzzy surface beams, $fs_{iv,ij:}$

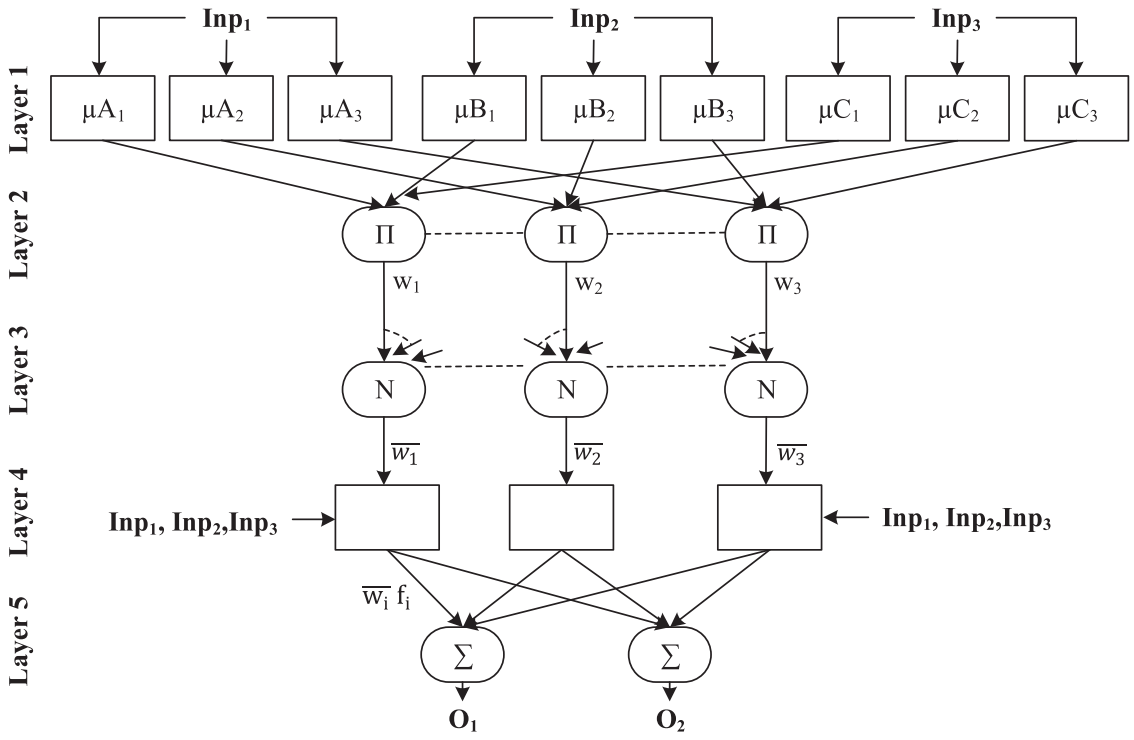

Fig. 3. CANFIS structure with three inputs and two outputs.

$_{ov}$, defined in Eq. (4) have been used.

$$fs_{iv,ij:ov}\left(PI_{iv:ov}, PI_{ij:ov}\right) = \frac{\sum_{k=1}^{M_{ov}} DWA_{k:ov} \bullet \mu_{iv,k:ov}\left(PI_{iv:ov}\right) \bullet \mu_{ij,k:ov}\left(PI_{ij:ov}\right)}{\sum_{k=1}^{M_{ov}} \mu_{iv,k:ov}\left(PI_{iv:ov}\right) \bullet \mu_{ij,k:ov}\left(PI_{ij:ov}\right)} \quad , \quad for\ ov = 1, \ldots, N_{ov} \tag{4}$$

where $PI_{iv:ov}$ and $PI_{ij:ov}$ are two potential input variables for output variable *ov*.

Then, similarly to Eq. (3), the MSE is computed for each fuzzy surface, $MSE_{fs_{iv,ij:ov}}$. Thus, fuzzy curves are initially used to rank all the potential input variables in ascending order. The PI variable with the smallest $MSEc_{iv,ov}$ is the most important input variable for each output variable *ov*. Fuzzy surfaces are then used to find the independent input variables and to eliminate the related input in each step (20% eliminated according to Lin et al., 1996). Therefore, in each step new fuzzy surfaces are computed and 20% of the potential input variable with the largest $MSE_{fs_{iv,ij:ov}}$ is eliminated.

3.2. Coactive neuro-fuzzy inference system (CANFIS)

A Coactive neuro-fuzzy inference system (CANFIS) is an extension of an adaptative network fuzzy inference system (ANFIS) (Jang et al., 1997) which integrates fuzzy inference systems (FISs) and artificial neural networks (ANNs) linked to a MIMO system, in the same methodology. CANFIS model can create different regions specialized in specific tasks such as different amount of water applied in different tariff period. FIS recreates the human thinking by a nonlinear relationship between inputs and outputs based on a set of "IF-THEN" rules. With the aim of making understandable the input variable to the rule set, the input variables are converted into linguistic variables by membership functions (MFs). Therefore, building a FIS consist of determining the MFs for each input variables as well as the rule set. The rule set and MFs form the knowledge base of the FIS.

On the other hand, the main drawback to obtain an optimal FIS is the lack of systematic procedures to determine its knowledge base. However, artificial neural networks can learn their structure from the input-output sets. Thus, in this work, under MIMO framework, a CANFIS model resulting from the combination of an ANN and a FIS was created to define the MF parameters. CANFIS can also find the rule base through the ANN learning ability to set the relationship between input and output. The typical structure of a CANFIS is made up by five layers (Fig. 3 where square nodes are adaptive nodes and circles nodes are fixed nodes) and their functions are described as follows:

The first layer (Layer 1) which is known as fuzzification layer uses the MFs to computes the outputs Out_n^l (*n* and *l* are the node and layer indexes, respectively). Each node *n* of this layer is a square node with a node function which is shown in Eq. (5) and 6. Each $Out_{n,i}^l$ corresponds to the *n*-th linguistic term of the *i*-th input variable Inp_i (e.g. the value of the variable *evapotranspiration* is 9.5 mm and it is turned into the linguistic term *the evapotranspiration is HIGH*)

$$Out_{n,i}^1 = \quad \mu_n\left(Inp_i\right) \tag{5}$$

Unlike previous works, in this work, the optimal typology of each MF will be determined by a GA. The different MF typologies considered during the optimization process will be described in section 2.4.

Every node in Layer 2 is a circle node labelled *Π*, which multiplies all the incoming signals (coming from Layer 1) and sends the product out to the next. This layer is known as firing strength, it contains the rule nodes, and it computes the activation value of each fuzzy rule, w_r, as Eq. (6):

$$Out_r^2 = w_r = \prod_{n=1}^{N_{input}} Out_{nm}^1 \quad \text{, for all the term nodes } m \text{ connected to the } r\text{-th rule node.}$$

$$r = 1, \ldots, N_{rules} \tag{6}$$

where N_{input} is the total number of inputs and N_{rules} is the total number of rules.

The third layer computes the rational firing strength of each nodes which is represented as circle node and labelled *N*. Thus, for convenience, outputs of this layer are called *normalized firing strengths* and they are computed according to the following equation:

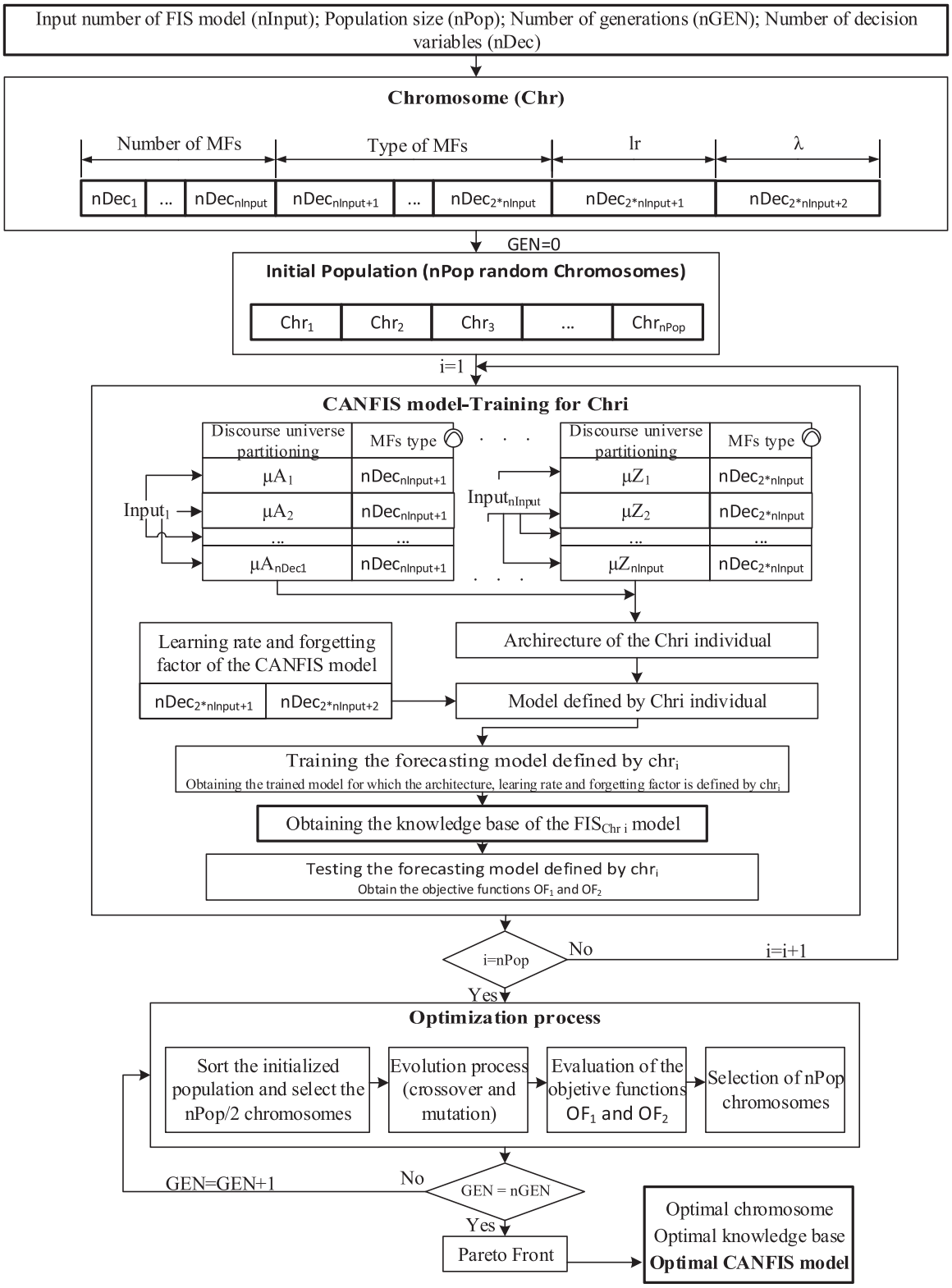

Fig. 4. Flowchart of the CANGENFIS model.

$$Out_r^3 = \overline{w_r} = \frac{Out_r^2}{\sum_{nr=1}^{N_{rules}} Out_{nr}^2}, \quad for \quad r = 1, \ldots, \quad N_{rules} \tag{7}$$

The defuzzification phase is carried out by Layer 4 (consequence parameters). Thus, the output of each node is the output of each *r*-th fuzzy rule that influences the *ov*-th model output Eq. (8).

$$Out_{r,ov}^4 = \overline{w_r} \cdot f_r^{ov} = \overline{w_r} \cdot \left(a_{1,r}^{ov} Inp_1 + a_{2,r}^{ov} Inp_2 + \ldots + a_{N_{input},r}^{ov} Inp_{N_{input}} + a_{0,r}^{ov} \right), \text{ for } r = 1, \ldots, N_{rules}, \ ov = 1, \ldots, N_{ov} \tag{8}$$

where $a_{1,r}^{ov}$, $a_{2,r}^{ov}$, ..., $a_{N_{input},r}^{ov}$, $a_{0,r}^{ov}$ are the consequent parameters of the

CANFIS system that represent the contribution of the *r*-th rule to the *ov*-th output.

Finally, in Layer 5 is represented as fixed node and labelled as $\sum$. In this layer, each *ov*-th model output is computed as the algebraic sum of the *ov*-th node's inputs Eq. (9).

$$Out_{ov}^{5} = \sum_{r}^{N_{rules}} Out_{r,ov}^{4}, \quad \text{for } ov = 1, \ldots, N_{ov} \tag{9}$$

Due to the complexity of the developed model and its computational efficiency, a first-order Takagi-Sugeno type of FIS was selected (Takagi and Sugeno, 1985), in this work. While, the antecedent part (*IF*) is always fuzzy, the consequent part (*THEN*) is a crisp linear function of an antecedent variable. Thus, three examples of typical first-order Takagi-Sugeno FIS rules are:

Rule 1.1: IF Inp_1 *is* A_1 *and* Inp_2 *is* B_1 *and* Inp_3 *is* C_1 *THEN* $f_{1,1} = a_{1,1}^{1}\, Inp_1 + a_{2,1}^{1}\, Inp_2 + a_{3,1}^{1}\, Inp_3 + a_{0,1}^{1}$.

Rule 1.2: IF Inp_1 *is* A_1 *and* Inp_2 *is* B_1 *and* Inp_3 *is* C_1 *THEN* $f_{1,2} = a_{1,1}^{2}\, Inp_1 + a_{2,1}^{2}\, Inp_2 + a_{3,1}^{2}\, Inp_3 + a_{0,1}^{2}$.

Rule 2.1: IF Inp_1 *is* A_2 *and* Inp_2 *is* B_2 *and* Inp_3 *is* C_2 *THEN* $f_{2,1} = a_{1,2}^{1}\, Inp_1 + a_{2,2}^{1}\, Inp_2 + a_{3,2}^{1}\, Inp_3 + a_{0,2}^{1}$.

Both the total number of rules and consequent parameters ($a_{1,1}^{1}$, $a_{2,1}^{1}$, …, $a_{0,2}^{1}$) will be automatically determined by the ANN during the training process of the CANFIS model.

In conventional ANNs, a simple back-propagation algorithm is usually used to train and adjust the weights which connects the neurons of different layers. In CAFIS structure, the parameters of the premises and consequents play the role of weights. The effectiveness of the developed FIS depends on these parameters. Thus, with the aim to improve the training process, Recursive Least Squares Estimation (RLSE) (Haykin, 2002) was used in this work as training algorithm of the CANFIS model. RLSE is an adaptive filter algorithm that recursively finds the coefficients ($a_{1,r}^{ov}$, $a_{2,r}^{ov}$, …, $a_{N_{input},r}^{ov}$, $a_{0,r}^{ov}$) that minimize a weighted linear least squares cost function relating to the model input. Although, this algorithm is computationally complex (its computational development has been implemented for this work), it has also extremely faster convergence than other training algorithm (Lewis and Hwang, 1990).

3.3. Coactive neuro-genetic fuzzy inference system (CANGENFIS)

The rule base and the MF parameters which defines the MF's shape is determined by an ANN in the CANFIS model. However, before defining the MF parameters, the number of MFs which defines each discourse universe of each input variable as well as the MF types that characterizes every linguistic label must be defined. CANFIS model is not able to automatically determine these essential variables for FIS and hence in most previous works are determined by trial and error without an optimization criterion. Thus, with the aim to optimize automatically both MFs number and the MF types, an hybrid model (*CANGENFIS*) which combines a CANFIS model and the multiobjective GA NSGA-II (Deb et al., 2002), has been developed in this work.

Furthermore, two essential parameters must be considered in the training process of the CANFIS model: *forgetting factor, λ,* which reduces the influence of old data in the determination of the synaptic weights of the CANFIS model (Haykin, 2002) and the *learning rate*, *lr*, which defines the updating rate of the MFs parameters (Hagan et al., 1996). Although, these parameters are highly sensitive in the accuracy of the forecasted model, standard values of these parameters are usually considered by most of the previous works, independently of the problem nature. In this work, these parameters are also optimized by the CANGENFIS model.

CANGENFIS model optimizes their decision variables (MFs number, MF types, λ and *lr*) based on two objective functions, OF_1 and OF_2. OF_1 maximizes the average of the determination coefficient of the model outputs (irrigation depth in each tariff periods) for the testing dataset of the CANGENFIS model. OF_2 minimizes the average and deviation of the standard error prediction (SEP) (Ventura et al., 1995) of the CANGENFIS. Standard deviation was considered to avoid the tendency to improve some specific outputs of the CANGENFIS model (e.g., forecasting of the irrigation depth applied in P6).

Table 1
Decision variables to be optimized during the optimization process of the CANGENFIS model.

Decision Variable	Gene	Range values	Description
Number of MFs	From 1 to *nInp*[a]	Integer values between 2 and 5	These genes determine the discourse universe division of each input variable.
Type of MFs	From *nInp* +1–2 *nInp*	Integer values between 1 and 4	These genes determine the shape of the MFs of each input variable:1: Generalized bell MF (gbellmf).2: Gaussian MF (gaussmf).3: Difference between two sigmoidal MF (dsigmf).4: Product of two sigmoidal MF (psigmf).
Learning rate (lr)	2 *nInp* +1	Values between 10^{-6} and 10^{-2}	This gene represents the learning rate of the optimization process of the CANGENFIS model.
Forgetting factor (λ)	2 *nInp* +2	Values between 0.95 and 1	This gene represents the forgetting factor of the optimization process of the CANGENFIS model.

[a] *nInput*: number of the input variables of the CANGENFIS model.

Fig. 4 shows the flow chart of the generation and optimization the CANGENFIS model. Initially, an initial population of *nPop* size is randomly generated. Each chromosome (*Chr*) or individual of the initial population is made up of *nDec* decision variables or genes that represent each hyperparameter of the CANGENFIS model to be optimized. In this work, the chromosome size is variable and depends on the number of inputs (*nInp*) to the forecasting model. Table 1 shows the decision variable (genes) considered in this work for *nInp* inputs in CANGENFIS model, as well as the value range that everyone can take during the optimization process. The first *nInp* genes determine the division of the discourse universe of each input variable of the predictive model. The next *nInp* genes define the type of the membership function of each input variable which transform the crisp input values into fuzzy input values and represent the activation function of the neurones of the first layer of CANGENFIS model. Learning rate and forgetting factor are represented by the last two genes, respectively.

Once the initial population is created (where the first *nInp*2* genes of each chromosome *chr* define the architecture of the *chr* model and the two last genes defines the complete chr model (architecture + learning way)), each individual of this population is trained and the knowledge base each forecasted model is obtained. After that, each of these trained models are tested and the objective function OF1 and OF2 are computed. Then, it is necessary to sort the initial population according to its aptitude, i.e., its forecast capacity (objective functions). The best *nPop/2* individuals are then selected as the best individual of the initial population. In the remaining stages, the *nPop/2* individuals are modified (crossover and mutation), and a new population of *nPop* individuals is generated. The process was repeated for several generations (*nGEN*). Finally, the set of *nPop* optimal individuals (optimal CANGENFIS models) obtained in the last generation defines the Pareto front.

The computational cost, mainly in computational time and memory, that the training process of each individual in each population required is hugely high. Thus, the number of epochs during the training phase of each forecast model must be limited. Consequently, at the end of the optimization process, the best models in terms of hyperparameters is obtained. However, the synaptic weights of the neural network (i.e. the knowledge base) are not yet optimized as it has not had enough time (enough training epochs) to adjust them. Hence, once the optimal models have been defined on the Pareto Front, they must be retrained without restriction of training epochs, obtaining the optimal knowledge base of the model.

Table 2
Potential inputs evaluated for CANGENFIS model.

Potential Input	Description
1	Number of hours of P1 in the day forecasted.
2	Number of hours of P2 in the day forecasted.
3	Number of hours of P3 in the day forecasted.
4	Number of hours of P4 in the day forecasted.
5	Number of hours of P5 in the day forecasted.
6	Number of hours of P6 in the day forecasted.
7	Daily maximum temperature (°C)
8	Daily average temperature (°C)
9	Daily minimum temperature (°C)
10	Daily maximum relative humidity (%)
11	Daily minimum relative humidity (%)
12	Daily average relative humidity (%)
13	Daily maximum wind speed (m s^{-1})
14	Daily average wind speed (m s^{-1})
15	Daily rainfall (mm)
16	Weekday
17	Farm area (ha)
18	Boolean holidays. This variable is equal to 1 for bank holidays and vacation days and 0 otherwise.
19	Applied irrigation dept, mm.
20	Month
21	Day of the year (DOI)

Table 3
Inputs selected for CANGENFIS model.

Potential Input id	Main Input	Description
1	MI_1	Number of hours of P1 in the day forecasted.
2	MI_2	Number of hours of P2 in the day forecasted.
6	MI_3	Number of hours of P6 in the day forecasted.
16	MI_4	Weekday
19	MI_5	Applied irrigation depth, mm.
21	MI_6	Day of the year (DOI)

4. Results and discussion

The methodology developed was applied to CZID during the 2015, 2016 and 2017 irrigation seasons to forecast one-day ahead the distribution in energy tariff periods of the irrigation depths applied at farm level by each farmer in the WUA. The complete dataset of irrigation depths applied contained a total of 77794 measures. Due to the differences of the irrigation practices for the main three crops and their impact on the applied irrigation depths (González Perea et al., 2018), the full dataset was classified according to the three main crops (rice, maize and tomato). Each of these datasets were randomly divided into two subsets: training dataset (80%) and testing dataset (20%).

The hyperparameters of the forecasting models were optimized by the multiobjective NSGA-II genetic algorithm. The number of individuals that must make up the initial population is related to the number and range of each gene. Thus, the random initial population (random CANGENFIS models) consisted of 100 individuals or chromosomes (*nPop*=100) for each one of the main crops. The number of generations depends on the stabilization time of each objective function. This stabilization is related to each problem and should not be pre-set, allowing the genetic algorithm to achieve its own stabilization. Consequently, the initial population was evolved for 300, 40 and 70 generations (*nGen* = 300, 40 and 70) for rice, maize and tomato, respectively where the values of OF_1 and OF_2 were stabilized. The probabilities for mutation and crossover were set to 10% and 90%, respectively.

4.1. Model inputs

The most important inputs for CANGENFIS model were selected from a set of 21 potential inputs following the methodology described in section 2.2. Table 2 shows the potential inputs evaluated and Table 3 shows the most important inputs selected. After applying the methodology of section 2.2., the most representative inputs and therefore the input variables of CANGENFIS model were number of hours of P1, P2 and P6 in the day to forecast, weekday, applied irrigation depth (mm) and day of the year (DOI). The applied irrigation depth of the day to be forecasted is an essential input for the model. When these models are working in real time (in a WUA), this input can be also obtained in real time using the previous model developed by González Perea et al. (2018).

As Table 3 shows the distribution in tariff period does not depends on any agroclimatic variables, not even the farm size or non-working days, contrarily to the previous works were these variables were essential to

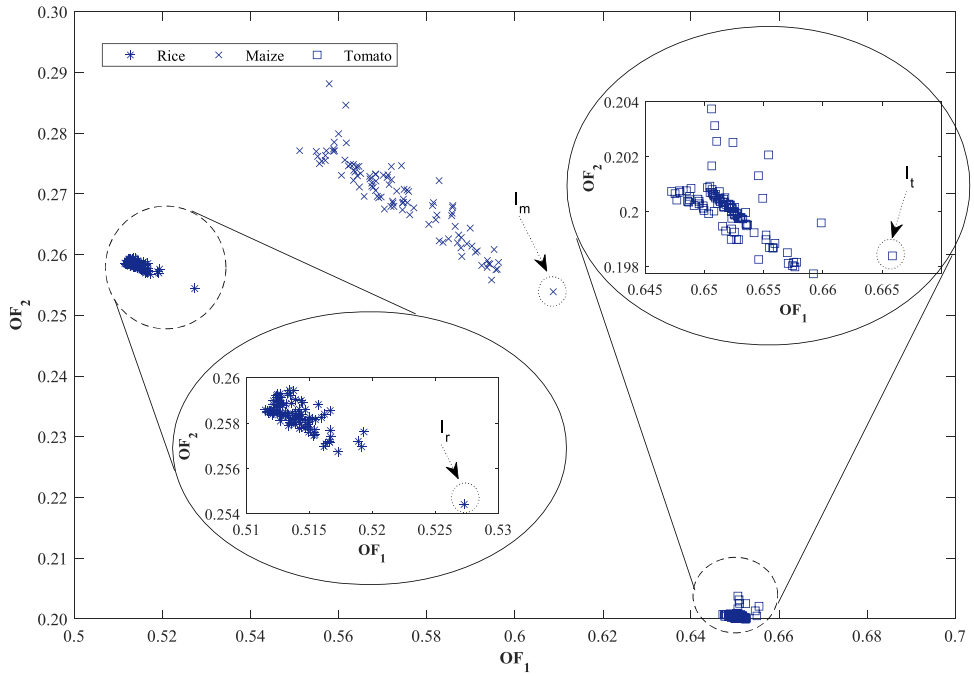

Fig. 5. Pareto fronts and best individuals (I_r, I_m, I_t) for rice, maize and tomato, respectively.

forecast the daily irrigation scheduling. These inputs highlight that the distribution in tariff period of the daily irrigation depth applied depends almost exclusively on hourly energy price of the tariff (Fig. 2). In other words, the distribution by tariff periods of the irrigation water applied depends more on the price of each tariff period than on the particularities or cultural habits of each farmer. Therefore, only information about the two expensive (P1 and P2) and the cheapest (P6) tariff periods (MI_1, MI_2 and MI_3, respectively) as well as the total amount of the irrigation water and the day of year and week (MI_4 and MI_6) is required.

4.2. Pareto front of the optimization process by GA

The modified Genetic algorithm NSGA-II optimized the objective functions, maximizing OF_1 and minimizing OF_2. The random initial population of 100 chromosomes or individuals evolved over 300, 40 and 70 generations for rice, maize and tomato, respectively. Each individual consisted of 14 genes ($2 \bullet nInput + lr + \lambda$) because the number of input variables (*nInput*) was 6.

Fig. 5 shows the Pareto fronts obtained in the last generation for rice (star mark), maize (cross mark) and tomato (square mark). This figure shows that the three crops are clearly different, obtaining the tomato model the best values of OF_1 and OF_2 (ranging from 0.647 to 0.666 and from 0.198 to 0.204 respectively). The OF_1 and OF_2 values ranged from 0.512 to 0.527 and from 0.254 to 0.26, respectively for the forecasting models developed for rice. Maize models obtained the widest range of values, their objective functions ranged from 0.551 to 0.61 for OF_1 and from 0.254 to 0.288 for OF_2. The three pareto fronts show that both objective functions are clearly in conflict. Consequently, as the representativeness of the predictive models represented by OF_1, the accuracy of the forecasting models represented by OF_2 decreased. This sensitivity of the models between accuracy and representativeness is much more pronounced in the models developed for maize crops as the slope of this pareto front is steeper than the other two.

Both the larger range of the values of the objective functions and the slope of the pareto front for the maize crop is relate to the number of generations during the optimization process. The maize model needed the lower number of generations to stabilize their objective functions. The methodology developed considered the effect of the random initial population over the evolution of the optimization process and a clock dynamic seed was programmed to avoid this effect in the evolution of the population. Therefore, the differences of the *nGen* value in the three crops are related to the nature of the problem, i.e. the differences in irrigation water management between crops, and not to an effect associated with random initiation of the initial population. Consequently, the maize model was easier to obtain than the other two crops. In addition, as reported by González Perea et al. (2018), the irrigation water management in this crop is easier to reproduce and better results can be obtained than in the other two crops. Due to the irrigation method (flood irrigation), rice is the crop that needed the most *nGen* value to stabilise their objective functions and the one with the worst values of accuracy and representativeness. This will be discussed below where the best model for each crop is analysed.

The architecture and the other hyperparameters of each model are defined by the values of each gene of each individual. The generalization ability of a model (capacity to reproduce previously unobserved events as in the test set) depends on these genes. The pareto fronts of rice and tomato did not show variation of the objective function values. This indicates that the number of training epochs was insufficient and these models did not have enough time to find the best values of their synaptic weights. Consequently, the values of the objective functions were insensitive to the different hyperparameters (genes) of each individual (each model). In order words, in rice and tomato's pareto fronts, the effect of the number of training epochs is more restrictive than the network architecture. However, the optimization process of the genetic algorithm does ensure that these individuals were the best (w.r.t the others analysed during the optimization process) and the fastest to train, even if further refinement of their synaptic weights is necessary.

Table 4
Gene values, R^2 and SEP values of the test set for I_r, I_m and I_t after refining models.

Gene	Input variable	Models		
		I_r[a]	I_m[b]	I_t[c]
Number of MFs	MI_1	3	3	3
	MI_2	3	3	3
	MI_3	3	3	3
	MI_4	3	3	3
	MI_5	2	2	3
	MI_6	3	2	2
Type of MFs	MI_1	Product of two sigmoidal	Difference between two sigmoidal	Difference between two sigmoidal
	MI_2	Product of two sigmoidal	Difference between two sigmoidal	Difference between two sigmoidal
	MI_3	Product of two sigmoidal	Difference between two sigmoidal	Difference between two sigmoidal
	MI_4	Difference between two sigmoidal	Difference between two sigmoidal	Difference between two sigmoidal
	MI_5	Product of two sigmoidal	Gaussian	Generalized bell
	MI_6	Gaussian	Difference between two sigmoidal	Difference between two sigmoidal
Learning rate (lr)		$3.89 \bullet 10^{-6}$	10^{-6}	$1.21 \bullet 10^{-3}$
Forgetting factor (λ)		0.9855	1	0.9775
R^2		0.70	0.76	0.85
SEP (%)		19.9	22.9	19.5

[a] Best forecasting model for rice crop.
[b] Best forecasting model for maize crop.
[c] Best forecasting model for tomato crop.

Table 5
Linguistic variables of each fuzzy set to partition each input variable for I_r, I_m and I_t models.

Input variable	Models		
	I_r[a]	I_m[b]	I_t[c]
Number of hours of P1 in the day forecasted.	HI/M/LO	HI/M/LO	HI/M/LO
Number of hours of P2 in the day forecasted.	HI/M/LO	HI/M/LO	HI/M/LO
Number of hours of P6 in the day forecasted.	HI/M/LO	HI/M/LO	HI/M/LO
Weekday	HI/M/LO	HI/M/LO	HI/M/LO
Applied irrigation depth, mm.	HI/LO	HI/LO	HI/M/LO
Day of the year (DOI)	HI/M/LO	HI/LO	HI/LO

LO: Low. M: Medium. HI: High.
[a] Best forecasting model for rice crop.
[b] Best forecasting model for maize crop.
[c] Best forecasting model for tomato crop.

Considering the values of each objective function, one individual per crop has been selected as the best one. Thus, Fig. 4 shows the best individual (the best forecasting model) from rice crop (I_r), maize crop (I_m) and tomato crop (I_t). These individuals will be analysed in the next Section.

4.3. Optimal CANGENFIS models

The best individual (CANGENFIS models) for each crop type in each pareto front was selected. Thus, I_r, I_m and I_t represents the best individual

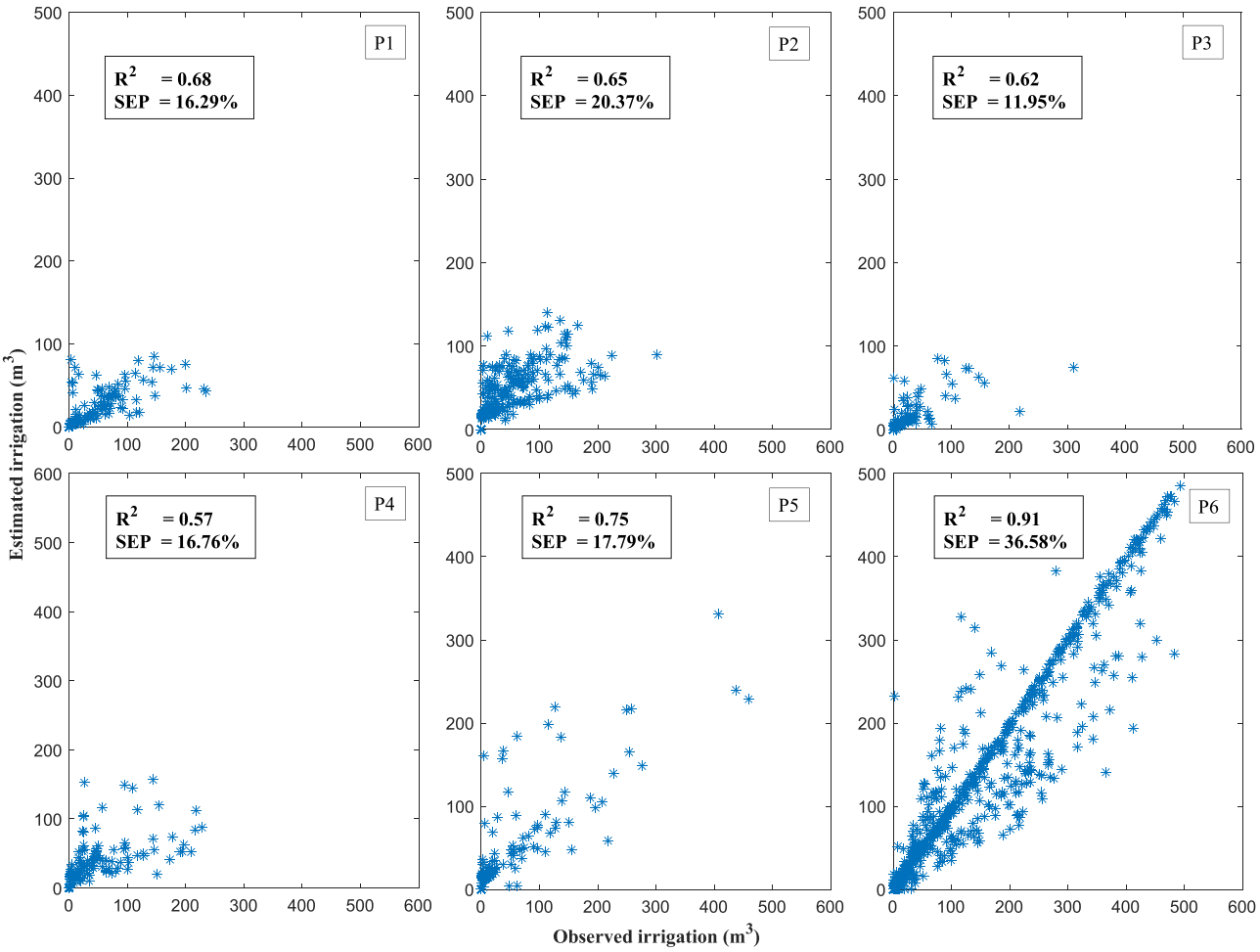

Fig. 6. Scatterplots between observed and estimated irrigation volume (test set) applied in each tariff period for I_r model.

for rice, maize and tomato, respectively. Table 4 shows the gene values that make up each CANGENFIS model as well as the R^2 and SEP values of the test set after the refining process without limitations of the number of training epochs. The partition of the discourse universe (Number of MFs) of each input variable was clearly stablished in 3 except for MI_5 in the rice model, MI_5 and MI_6 in the maize model and MI_6 in the tomato model. The minimum and maximum values that these genes would take ranged from 2 to 5. For no input variable in any developed model (I_r, I_m and I_t), these genes corresponding to the partitions of their discourse universe tended to their maximum values (these genes could range from 2 to 5). Consequently, the range of values for these genes during the optimization process was properly established. A tendency towards any of the lower or upper limits would indicate the need to modify this range and repeat the optimization process of the genetic algorithm.

Table 5 shows the linguistic variables for each one of the partitions of the discourse universe of each input variable for the three models assessed. In the three models, the number of hours in P1, P2 and P6 (MI1, MI2 and MI3, respectively) in the forecasted day were addressed in the same way for farmers who irrigate rice, maize or tomato. Thus, the linguistic variables or the reasoning that all farmers consider about the distribution of these hours for every day as high (HI), medium (M) or low (LO), i.e., the behaviour of each farmer in the WUA in deciding how to apply the irrigation depth on a given day is conditioned by whether the number of hours available is high, medium or low for the two most expensive tariff period (P1 and P2) and the cheapest period (P6). Similarly, for all farmers the week is divided into early week (LO), mid-week (M) and late week (HI). It is reasonable that the partition of the discourse universe for this variable would have been 2 (weekend and all other days) since the distribution of the tariff periods is conditioned by weekends (Fig. 2). However, the results for this input variable (MI_4) show that it is also important whether the farmer is at the beginning or in the middle of the week, possibly conditioned by his activity during the weekend and some other socio-cultural practices that should be studied in detail. The applied irrigation depth (MI_5) was processed differently for rice and maize than for tomato. While for rice and maize considers high (H) or low (L) irrigation depths, for tomato high (H), medium (M) or low (L) irrigation depths are considered. The irrigation season was also divided differently depending on the crop type. The decision of the distribution of the daily applied irrigation depth is conditioned whether DOI (MI_6) is at the beginning, middle or end of the irrigation season for rice. However, for maize and tomato, the irrigation season was divided into early or late. This way of considering the irrigation season is related to the irrigation system of each crop (rice is irrigated by flooding, maize and tomato by drip irrigation). I.e., farmers with rice irrigated by flooding and vary their irrigation management according to three periods of the irrigation season (beginning, middle and end). However, the irrigation management of farmers with tomato and maize is affected only by two periods along the irrigation season. This division of the irrigation season has not only been caused by the irrigation method but also the different phenological stages of each crop.

Table 4 also shows the type of MFs for each input variable and each model. The crop cycle, the irrigation system and the daily irrigation depths to be applied in rice differ greatly from maize and tomato. Consequently, the way in which the knowledge base of the fuzzy inference system of each CANGENFIS model transforms the crisp input values into linguistic variables (fuzzy values) is very similar for maize

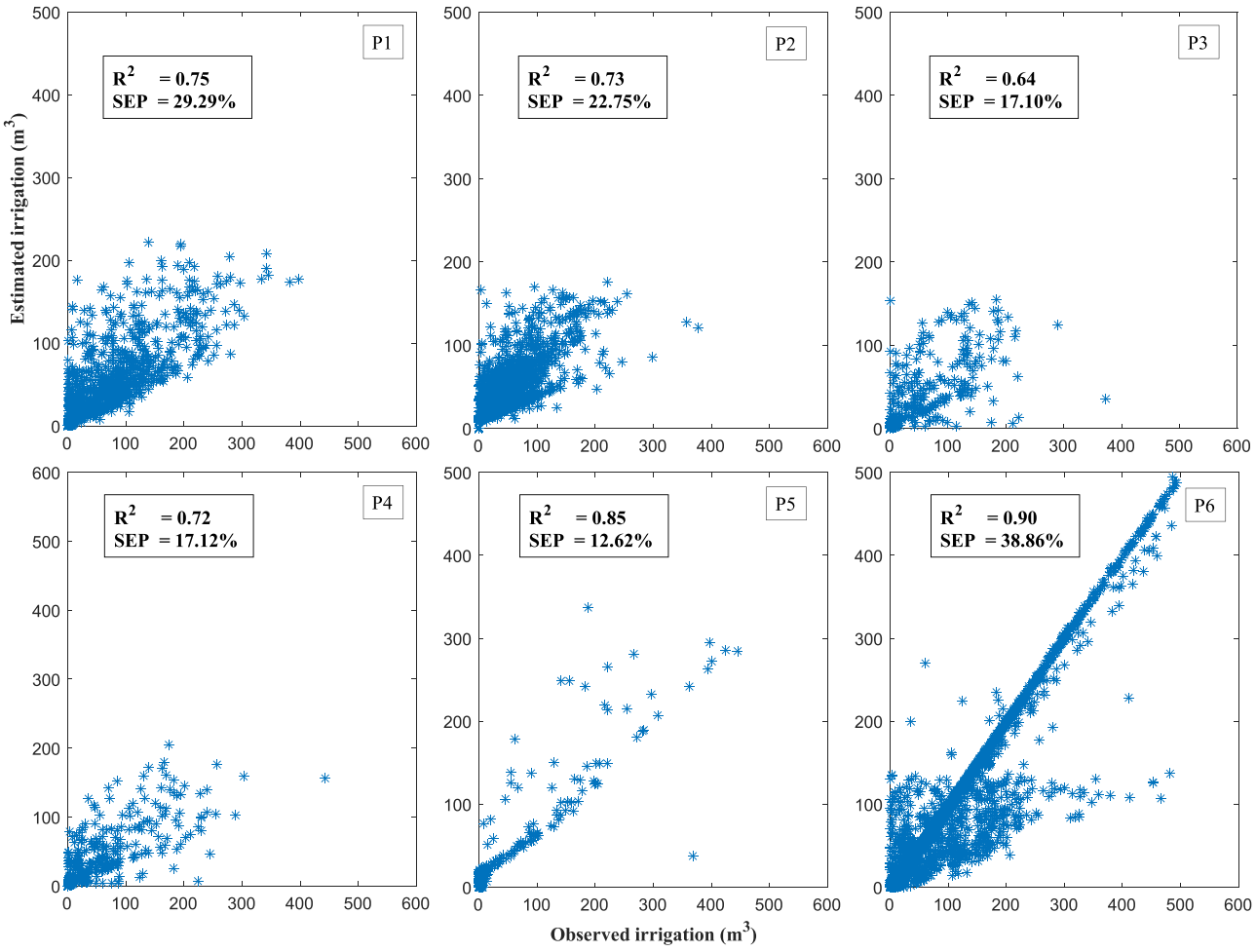

Fig. 7. Scatterplots between observed and estimated irrigation volume (test set) applied in each tariff period for I_m model.

and tomato, moving away from the behaviour for rice. Apart from the days of the week (MI_4), the knowledge base of the rice model is totally different from the other two models. The values of learning rate were $3.89 \cdot 10^{-6}$, 10^{-6} and $1.21 \cdot 10^{-3}$ for I_r, I_m and I_t, respectively. The optimal *lr* value depends on the shape of the N-dimensional error function or cost function between the target value and the forecasted values during the training process. Thus, in those error functions, where the decreasing error path can clearly be found, it is possible to increase the value of *lr*, speeding up the training process. However, the error functions with more tortuous paths to their global minima cannot have very high *lr* value as they would not find this minimum value. Results show that the N-dimensional space of the error function of I_t model is less tortuous and easier to find an optimal point than the others due to it achieved the lower value of *lr*. Contrary, I_m obtained the lower value of *lr*. Forgetting factor is a hyperparameter of the training function used in this work (RLS): This hyperparameter defines the amount of information which is forgotten in each step of the recursive training process. The smaller value of λ, the smaller is the contribution of previous sample to the covariance matrix of the RLS algorithm. This makes the algorithm more sensitive to recent samples, or recent records rather than older ones. Thus, the λ values for I_r, I_m and I_t were 0.9855, 1 and 0.9775, respectively. I_m model is the only that obtain a value of 1 for this hyperparameter. When the forgetting factor is 1, it is referred to as the growing window RLS algorithm.

The representativeness and the accuracy of the three models selected are defined by the R^2 and SEP values and it also shows in Table 4. The R^2 values for I_r, I_m and I_t were 0.70, 0.76 and 0.85, respectively. The SEP values for these three models were 19.9%, 22.9% and 19.5%, respectively. Thus, the I_t model was the most accurate, with the highest representativeness and lower error than 20% for 85% of the forecasting. As González Perea et al. (2018) shown in their results, the rice model is the most complex, probably because their irrigation system and the amount of data for this crop type. Consequently, this work confirms these findings and also obtains the lowest representativeness although the accuracy was lower than 20%. However, the three models are MIMO, i.e. each model receives the input variable (from MI1 to MI6) and return the distribution the applied irrigation depth in a day *d* for each tariff period (from P1 to P6). Thus, the R^2 and SEP values are an average of the six outputs of each model. Figs. 6–8 shows the scatterplots between observed and estimated irrigation water for the test dataset for the models I_r, I_m and I_t, respectively. For I_r, the R^2 values ranged from 0.57 for P4 to 0.91 for P6. However, the SEP values ranged from 36.58% in P6 to 11.95% in P3. Similarly, the R^2 values for I_m and I_r models ranged from 0.64 in P4 to 0.90 in P6 and from 0.82 in P2 to 0.94 in P6, respectively. The SEP values for these two models ranged from 38.86% in P6 to 12.62% in P5 and from 30.94% in P6 to 12.13% in P5, respectively. For the three models, the highest R^2 value was obtained in P6 but with the highest SEP value. Contrary, the lowest SEP value was found in P5 for I_m and I_t models and in P3 for I_r model. Figs. 6–8 also show that most of the irrigation water is logically applied in the cheapest tariff period (P6). Also, larger farms with highest irrigation water inputs (higher volume of irrigation water applied) trend to maximize the input in the cheapest period. Consequently, the most expensive tariff period (P1) hardly exceeds 200 m^3 per irrigation event with more than 95% of the tomato and maize farms are less than 5 ha and no rice farms are larger than 8 ha (only 3 farms between 5 ha and 8 ha). It is important to

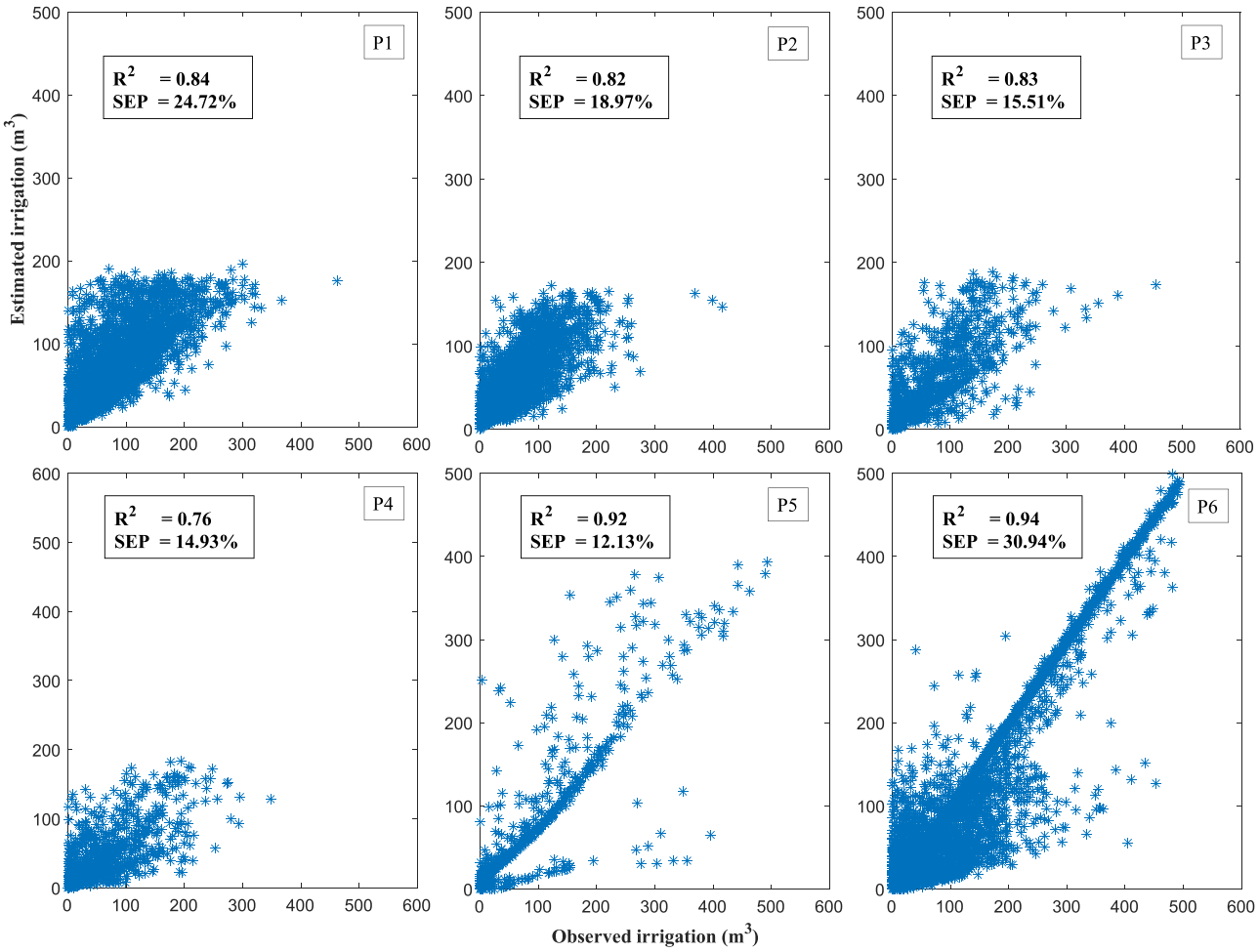

Fig. 8. Scatterplots between observed and estimated irrigation volume (test set) applied in each tariff period for I_t model.

highlight that Figs. 6–8 show how the second cheapest tariff period (P5) is the one that receives less irrigation water when intuitively it should be the second period receiving more water. This is a consequence of the distribution of the tariff periods (Fig. 2) throughout the irrigation season. While P6 is in one of the months of the irrigation season with highest crop water requirements, P5 is at the beginning and end of the irrigation season when the theoretical irrigation requirements are smaller. These asymmetric distribution of the irrigation water between the tariff periods are responsible for the variation in the R^2 and SEP values between tariff periods. As the architecture of the three models have been adapted and optimized for these conditions, as more records are obtained in each of these tariff periods, the models will learn and improve their accuracy in an autonomous and automatic way.

5. Conclusions

The prediction of irrigation events occurrence and applied irrigation depths was previously addressed in previous works. However, the optimization of irrigation water use and the energy contracting requires also the knowledge of their distribution throughout the day. Thus, a new hybrid methodology (CANGENFIS) combining multiple-inputs multiple outputs, fuzzy logic, artificial neural networks and multiobjective genetic algorithms has been developed to forecast the intra-daily distribution of each irrigation event. The new methodology developed in Matlab was applied to a real WUA and three models were calibrated for rice, maize and tomato. Although some differences between tariff periods were observed, the R^2 and SEP values for the three models were 0.70, 0.76% and 0.85% and 19.9% 22.9% and 19.5%, respectively.

CANGENFIS also optimized the inputs of the three forecasting models following fuzzy logic techniques. Contrarily to the forecasting of daily water demand, the distribution by tariff periods did not depend on any agroclimatic variables. These findings highlight that the hourly distribution of the daily irrigation events depend almost exclusively on tariff periods according to their price.

Finally, these models provide the amount of water that each farmer of the WUA is going to apply in each energy tariff period one day ahead. The aggregation of this information for the total number of farmers in the WUA provides the total amount of water one day in advance but discriminated by energy tariff period. In addition, the farms are geo-positioned so managers will know in advance which pipes can be overloaded. Thus, with these models, the manager have an overview about the circulating flows in the network the day after but also the distribution of water demand and therefore the power requirements in each tariff period could be estimated. This information can be very valuable for the optimum contracting of the electricity tariff with the supplying company.

Declaration of Competing Interest

The authors declare that they have no known competing financial interests or personal relationships that could have appeared to influence the work reported in this paper.

Acknowledgments

This research is funded by the Spanish Ministry of Economy and

Competitiveness through the AGL2017-82927-C3-1-R Project. We acknowledge financial support from the Spanish Ministry of Science and Innovation, the Spanish State Research Agency, through the Severo Ochoa and María de Maeztu Program for Centers and Units of Excellence in R&D (Ref. CEX2019-000968-M).

References

Agarwal, A., Mishra, S.K., Ram, S., Singh, J.K., 2006. Simulation of runoff and sediment yield using artificial neural networks. Biosyst. Eng. 94, 597–613. https://doi.org/10.1016/j.biosystemseng.2006.02.014.

Anctil, F., Rat, A., 2005. Evaluation of neural network streamflow forecasting on 47 watersheds. J. Hydrol. Eng. 10, 85–88. https://doi.org/10.1061/(ASCE)1084-0699(2005).

Bazilian, M., Rogner, H., Howells, M., Hermann, S., Arent, D., Gielen, D., Steduto, P., Mueller, A., Komor, P., Tol, R.S.J., Yumkella, K.K., 2011. Considering the energy, water and food nexus: towards an integrated modelling approach. Energy Policy 39, 7896–7906. https://doi.org/10.1016/j.enpol.2011.09.039.

Bin, H.X., Xin, Z.H., 2013. Build enterprise competitive intelligence system model based on Big Data. J. Intell. 3, 37–43.

Conforti, P., 2011. Looking Ahead in World Food and Agriculture: Perspectives to 2050. Food and Agriculture Organization, Rome.

Corominas, J., 2010. Agua y energía en el riego en la época de la sostenibilidad. Ing. Agua 17, 219–233.

Deb, K., Pratap, A., Agarwal, S., Meyarivan, T., 2002. A fast and elitist multiobjective genetic algorithm: NSGA-II. IEEE Trans. Evol. Comput. 6, 182–197.

EEA, (European Enviromental Agency), 2012. Towads efficient use of water resources in Europe, EEA Rep. 1/2012.

González Perea, R., 2017. Optimum Management of Pressurized Irrigation Networks at Different Scales Using Artificial Intelligent Techniques. University of Cordoba.

González Perea, R., Camacho Poyato, E., Montesinos, P., Rodríguez Díaz, J.A., 2018. Prediction of applied irrigation depths at farm level using artificial intelligence techniques. Agric. Water Manag. 206, 229–240. https://doi.org/10.1016/j.agwat.2018.05.019.

González Perea, R., Poyato, E.C., Montesinos, P., Diaz, J.A.R., 2015. Irrigation demand forecasting using artificial neuro-genetic networks. Water Resour. Manag. 29, 5551–5567.

Hagan, M.T., Demuth, H.B., Beale, M.H., 1996. Neural Network Design. PWS Publishing Co., Boston, Massachusetts.

Haykin, S., 2002. Adaptive Filtering Theory. Prentice-Hall.

Hunt, C.E., 2004. Thristy Plant-Strategies for Sustainable Water Management. Bloomsbury, New York.

Jang, J.-S.R., Sun, C.-T., Mizutani, E., 1997. Neuro-Fuzzy And Soft Computing Jang. Prentice-Hall, USA.

Lewis, P.S., Hwang, J.N., 1990. Recursive least-squares learning algorithms for neural networks 1348, 28–39. https://doi.org/10.1117/12.23462.

Lin, Y., Cunningham III, G.A., Coggeshall, S.V., 1996. Input variable identification—fuzzy curves and fuzzy surfaces. Fuzzy Sets Syst. 82, 65–71.

MARM, M. of E. and R. and M.A., 2010. National Strategy for Sustainable Modernization of Irrigation-Horizon 2015.

Ondimu, S., Murase, H., 2007. Reservoir level forecasting using neural networks: Lake Naivasha. Biosyst. Eng. 96, 135–138. https://doi.org/10.1016/j.biosystemseng.2006.09.003.

Plusquellec, H., 2009. Modernization of large-scale irrigation systems: is it an achievable objective or a lost cause. Irrig. Drain. 58, S104–S120.

Pulido-Calvo, I., Gutiérrez-Estrada, J.C., 2009. Improved irrigation water demand forecasting using a soft-computing hybrid model. Biosyst. Eng. 102, 202–218. https://doi.org/10.1016/j.biosystemseng.2008.09.032.

Rezaei, F., Safavi, H.R., Zekri, M., 2017. A hybrid fuzzy-based multi-objective PSO algorithm for conjunctive water use and optimal multi-crop pattern planning. Water Resour. Manag. 31, 1139–1155. https://doi.org/10.1007/s11269-016-1567-4.

Takagi, T., Sugeno, M., 1985. Fuzzy identification of systems and its applications to modeling and control. IEEE Trans. Syst. Man Cybern. SMC-15, 116–132. https://doi.org/10.1109/TSMC.1985.6313399.

Ventura, S., Silva, M., Pérez-Bendito, D., Hervás, C., 1995. Artificial neural networks for estimation of kinetic analytical parameters. Anal. Chem. 67, 1521–1525.